Survey on Symplectic Finite-Difference Time-Domain Schemes for Maxwell's Equations

Wei Sha, Zhixiang Huang, Mingsheng Chen, and Xianliang Wu

Abstract—To discretize Maxwell's equations, a variety of high-order symplectic finite-difference time-domain (p, q) schemes, which use pth-order symplectic integration time stepping and qth-order staggered space differencing, are surveyed. First, the order conditions for the symplectic integrators are derived. Second, the comparisons of numerical stability, dispersion, and energy-conservation are provided between the high-order symplectic schemes and other high-order time approaches. Finally, these symplectic schemes are studied by using different space and time strategies. According to our survey, high-order time schemes for matching high-order space schemes are required for optimum electromagnetic simulation. Numerical experiments have been conducted on radiation of electric dipole and wideband S-parameter extraction of dielectric-filled waveguide. The results demonstrate that the high-order symplectic scheme can obtain satisfying numerical solutions under high Courant–Friedrichs–Levy number and coarse grid conditions.

Index Terms—High-order differences, Maxwell's equations, numerical stability and dispersion, symplectic integrators.

I. INTRODUCTION

AS THE MOST standard algorithm, the traditional finite-difference time-domain (FDTD) method [1], [2], which is explicit second-order accurate in both space and time, has been widely applied to electromagnetic computation and simulation. One of the primary drawbacks associated with the FDTD method is the significant accumulated errors from numerical instability, dispersion and anisotropy. Hence, fine grids must be used to obtain satisfying numerical results, which leads to vast memory requirements and high computational costs, especially for electrically-large domains and for long-term simulation.

To overcome the shortcoming, some high-order space strategies have been put forward. For example, Fang proposed the high-order FDTD(4,4) method [3]. Yet, the method is difficult to handle material interface for modeling the three-dimensional complex objects. Another approach is the staggered FDTD(2,4) method [4]–[6]. However, the method must set lower Courant–Friedrichs–Levy (CFL) number to obtain high-order numerical precision.

In order to further explore efficient methods for optimum electromagnetic simulation, other improved time strategies are

proposed. For example, the high-order Runge-Kutta (R-K) approach was introduced in [7]–[9]. However, the approach is dissipative and needs large amount of memory. Another alternative method is the alternating direction implicit FDTD (ADI-FDTD) algorithm [10], [11]. Although it saves CPU time owing to unconditional stability, undesirable numerical precision and dispersion will happen once the high CFL number is adopted.

Based on the assumption that Maxwell's equations can be written as infinite-dimensional Hamiltonian system [12], the energy-preserving explicit symplectic integration scheme has been introduced to the computational electromagnetics [13], [14]. Although it is nondissipative and saves memory, the symplectic FDTD (SFDTD) scheme proposed in [13] needs at least four iterations within every time step compared with one iteration for the traditional FDTD method. As a result, the SFDTD scheme with higher stability and lower dispersion does not seem to acquire lower computational complexity. To solve the problem, the optimized symplectic integrators are constructed in [15], [16], but they are only second-order accurate in time, and equivalent to the leap-frog time integration method.

The problems of interest here are how to construct optimized high-order symplectic integrators, and how to verify the advantages of them over low-order symplectic integrators and over other high-order time strategies. On the one hand, we derive the order conditions for constructing the optimized high-order symplectic integrators, and propose an averaged stability limit criterion for analyzing the computational complexity of them. On the other hand, with different symplectic integrators and spatial differences, the SFDTD schemes are studied and compared.

II. SYMPLECTIC FRAMEWORK FOR MAXWELL'S EQUATIONS

A function of space and time evaluated at a discrete point in the Cartesian lattice and at a discrete stage in the time step can be notated as

$$F(x, y, z, t) = F^{n+l/m} (i\Delta_x, j\Delta_y, k\Delta_z, (n + \tau_l)\Delta_t) \quad (1)$$

where Δ_x, Δ_y, and Δ_z are, respectively, the lattice space increments in the x, y, and z coordinate directions, Δ_t is the time increment, $i, j, k, n, l,$ and m are integers, $n + l/m$ denotes the lth stage after n time steps, m is the total stage number, and τ_l is the fixed time with respect to the lth stage.

For the spatial direction, the explicit qth-order accurate centered difference expressions in conjugation with the staggered Yee lattice are used to discretize the first-order spatial derivatives, shown in (2) at the bottom of the following page, where $\delta = x, y, z$, $h = i, j, k$, and W_r are the coefficients of spatial differences. W_s is defined as $W_s = 2 \times \sum_{r=1}^{q/2} |W_r|$, and the

The authors are with the Key Laboratory of Intelligent Computing and Signal Processing, Anhui University, Hefei 230039, China (e-mail: ws108@ahu.edu.cn; xlwu@ahu.edu.cn).

TABLE I
COEFFICIENTS OF qth-ORDER ACCURATE CENTERED DIFFERENCES

Order (q)	W_1	W_2	W_3	W_4	W_s
2	1				2
4	9/8	−1/24			7/3
6	75/64	−25/384	3/640		149/60
8	1225/1024	−245/3072	49/5120	−5/7168	2161/840

values of W_r and the computed W_s are listed in Table I. From the table, W_s increases as the order of differences increases.

For the temporal direction, Maxwell's equations in homogeneous, lossless, and sourceless medium can be written as [13]

$$\frac{\partial}{\partial t}\begin{pmatrix} \mathbf{H} \\ \mathbf{E} \end{pmatrix} = (U + V)\begin{pmatrix} \mathbf{H} \\ \mathbf{E} \end{pmatrix} \tag{3}$$

$$U = \begin{pmatrix} \{0\}_{3\times3} & -\mu^{-1}\{R\}_{3\times3} \\ \{0\}_{3\times3} & \{0\}_{3\times3} \end{pmatrix}_{6\times6}$$

$$V = \begin{pmatrix} \{0\}_{3\times3} & \{0\}_{3\times3} \\ \varepsilon^{-1}\{R\}_{3\times3} & \{0\}_{3\times3} \end{pmatrix}_{6\times6} \tag{4}$$

$$R = \begin{pmatrix} 0 & -\frac{\partial}{\partial z} & \frac{\partial}{\partial y} \\ \frac{\partial}{\partial z} & 0 & -\frac{\partial}{\partial x} \\ -\frac{\partial}{\partial y} & \frac{\partial}{\partial x} & 0 \end{pmatrix} \tag{5}$$

where $\{0\}_{3\times3}$ is the 3×3 null matrix, R is the three-dimensional curl operator, and ε and μ are the permittivity and the permeability of the medium.

Using the product of elementary symplectic mapping, the exact solution of (3) from $t = 0$ to $t = \Delta_t$ can be approximately constructed [17]

$$\exp\left(\Delta_t(U+V)\right) = \prod_{l=1}^{m} \exp(d_l\Delta_t V)\exp(c_l\Delta_t U) + O\left(\Delta_t^{p+1}\right) \tag{6}$$

where c_l and d_l are the symplectic integrators. Accordingly, the m stage and pth-order symplectic scheme is constructed. Generally, $m \geq p$.

In view of $U^\alpha = 0, \alpha \geq 2$ and $V^\alpha = 0, \alpha \geq 2$, we can employ Taylor series to expand the right-hand side of (6) into the matrix form

$$\begin{pmatrix} I_{3\times3} & \{0\}_{3\times3} \\ d_m\Delta_t v_{3\times3} & I_{3\times3} \end{pmatrix}\begin{pmatrix} I_{3\times3} & c_m\Delta_t u_{3\times3} \\ \{0\}_{3\times3} & I_{3\times3} \end{pmatrix}\cdots$$
$$\begin{pmatrix} I_{3\times3} & \{0\}_{3\times3} \\ d_1\Delta_t v_{3\times3} & I_{3\times3} \end{pmatrix}\begin{pmatrix} I_{3\times3} & c_1\Delta_t u_{3\times3} \\ \{0\}_{3\times3} & I_{3\times3} \end{pmatrix} \tag{7}$$

where $u_{3\times3} = -\mu^{-1}\{R\}_{3\times3}$, $v_{3\times3} = \varepsilon^{-1}\{R\}_{3\times3}$, and I is the 3×3 unit matrix.

Similarly, the left-hand side of (6) can be written in (8), shown at the bottom of the page, where $p = 2\beta, \beta \in N$.

$$\left(\frac{\partial F^{n+l/m}}{\partial \delta}\right)_h = \sum_{r=1}^{q/2} W_r \frac{F^{n+l/m}(h+r-1/2) - F^{n+l/m}(h-r+1/2)}{\Delta_\delta} + O\left(\Delta_\delta^q\right) \tag{2}$$

$$\{I\}_{6\times6} + \Delta_t(U_{6\times6} + V_{6\times6}) + \frac{\Delta_t^2}{2!}(U_{6\times6}V_{6\times6} + V_{6\times6}U_{6\times6}) + \frac{\Delta_t^3}{3!}(U_{6\times6}V_{6\times6}U_{6\times6} + V_{6\times6}U_{6\times6}V_{6\times6}) + \cdots$$
$$+ \frac{\Delta_t^p}{p!}(\overbrace{U_{6\times6}V_{6\times6}U_{6\times6}\ldots V_{6\times6}}^{p} + \overbrace{V_{6\times6}U_{6\times6}V_{6\times6}\cdots U_{6\times6}}^{p})$$
$$+ \frac{\Delta_t^{p+1}}{(p+1)!}(\overbrace{U_{6\times6}V_{6\times6}U_{6\times6}V_{6\times6}\cdots U_{6\times6}}^{p+1} + \overbrace{V_{6\times6}U_{6\times6}V_{6\times6}U_{6\times6}\cdots V_{6\times6}}^{p+1}) + \cdots$$
$$= \begin{pmatrix} I_{3\times3} & \{0\}_{3\times3} \\ \{0\}_{3\times3} & I_{3\times3} \end{pmatrix} + \Delta_t\begin{pmatrix} \{0\}_{3\times3} & u_{3\times3} \\ v_{3\times3} & \{0\}_{3\times3} \end{pmatrix} + \frac{\Delta_t^2}{2!}\begin{pmatrix} u_{3\times3}v_{3\times3} & \{0\}_{3\times3} \\ \{0\}_{3\times3} & v_{3\times3}u_{3\times3} \end{pmatrix}$$
$$+ \frac{\Delta_t^3}{3!}\begin{pmatrix} \{0\}_{3\times3} & u_{3\times3}v_{3\times3}u_{3\times3} \\ v_{3\times3}u_{3\times3}v_{3\times3} & \{0\}_{3\times3} \end{pmatrix} + \cdots + \frac{\Delta_t^p}{p!}\begin{pmatrix} \overbrace{u_{3\times3}v_{3\times3}u_{3\times3}\cdots v_{3\times3}}^{p} & \{0\}_{3\times3} \\ \{0\}_{3\times3} & \underbrace{v_{3\times3}u_{3\times3}v_{3\times3}\cdots u_{3\times3}}_{p} \end{pmatrix}$$
$$+ \frac{\Delta_t^{p+1}}{(p+1)!}\begin{pmatrix} \{0\}_{3\times3} & \overbrace{u_{3\times3}v_{3\times3}u_{3\times3}v_{3\times3}\cdots u_{3\times3}}^{p+1} \\ \underbrace{v_{3\times3}u_{3\times3}v_{3\times3}u_{3\times3}\cdots v_{3\times3}}_{p+1} & \{0\}_{3\times3} \end{pmatrix} + \cdots \tag{8}$$

TABLE II
TIME-REVERSIBLE SYMPLECTIC INTEGRATORS: $c_l = c_{m-l+1}(1 \leq l \leq m)$, $d_l = d_{m-l}(1 \leq l \leq m-1)$, AND $d_m = 0$

Order (p)	Stage (m)	c_1	c_2	c_3	d_1	d_2	λ_T
*2	2	0.5	c_1		1	0	2.000
2	3	$(1/2 - \sqrt{3}/6)$	$\sqrt{3}/3$	c_1	1/2	d_1	2.632
2	3	1/6	2/3	c_1	1/2	d_1	2.450
2	3	$1/2 + \sqrt{3}/6$	$-\sqrt{3}/3$	c_1	1/2	d_1	1.593
*4	5	0.16537923	1.35491814	-2.04059474	0.51541261	-0.01541261	3.467
4	4	0.67560359	-0.17560359	c_2	1.35120719	-1.70241438	1.573
4	5	0.77751818	-0.54407885	0.53312134	1.02979385	-0.52979385	1.298

TABLE III
HALF-UNITARY SYMPLECTIC INTEGRATORS: $d_l = c_{m-l+1}(1 \leq l \leq m)$

Order (p)	Stage (m)	c_1	c_2	c_3	c_4	λ_T
2	2	$1 - \sqrt{2}/2$	$\sqrt{2}/2$			2.265
2	2	$1 + \sqrt{2}/2$	$-\sqrt{2}/2$			0.828
*3	3	0.26833010	-0.18799162	0.91966152		4.520
3	3	1.99505719	0.70009915	-1.69515634		0.912
4	4	0.11189654	0.70350157	-0.14654317	0.33114506	3.238
4	4	0.70963113	0.24786114	-0.96247655	1.00498428	1.695
4	4	-11.77866774	13.41348887	-0.63843697	0.00361584	1.096
4	4	2.13492775	1.82345122	-0.69563510	-2.26274387	0.495

Then we compare the coefficients of the Δ_t^p terms of (7) and (8), the pth-order conditions can be derived as follows:

$p = 2\beta - 1, \beta \in N$

$$\sum c_{l_1} d_{l_2} c_{l_3} d_{l_4} \cdots c_{l_p} = \frac{1}{p!}$$
$$1 \leq l_1 \leq l_2 < l_3 \leq l_4 < \cdots < l_p \leq m \quad (9)$$

$$\sum d_{l_1} c_{l_2} d_{l_3} c_{l_4} \cdots d_{l_p} = \frac{1}{p!}$$
$$1 \leq l_1 < l_2 \leq l_3 < l_4 \leq \cdots \leq l_p \leq m \quad (10)$$

$p = 2\beta, \beta \in N$

$$\sum c_{l_1} d_{l_2} c_{l_3} \cdots d_{l_p} = \frac{1}{p!}$$
$$1 \leq l_1 \leq l_2 < l_3 \leq \cdots \leq l_p \leq m \quad (11)$$

$$\sum d_{l_1} c_{l_2} d_{l_3} \cdots c_{l_p} = \frac{1}{p!}$$
$$1 \leq l_1 < l_2 \leq l_3 < \cdots < l_p \leq m. \quad (12)$$

Unfortunately, the equations [(9)–(12)] are not independent of each other, the time-reversible [17] or half-unitary [18] constraint must be employed such as

$$c_l = c_{m-l+1}(1 \leq l \leq m),$$
$$d_l = d_{m-l}(1 \leq l \leq m-1), \ d_m = 0 \quad (13)$$
$$d_l = c_{m-l+1}(1 \leq l \leq m). \quad (14)$$

The pth-order symplectic integrators must satisfy (**A**) from first-order conditions to pth-order conditions; (**B**) time-reversible constraint (13) or half-unitary constraint (14). Even so, for time-reversible symplectic integrators, there is still an unknown that cannot be solved. So we force the time-reversible symplectic integrators to satisfy (**C**) any one of the $(p+1)$th-order conditions.

From (A-C), the optimized symplectic integrators listed in Tables II and III can be obtained. Noticeably, the time-reversible symplectic integrators in [13] only satisfy (A) and (B) but not (C).

III. STABILITY ANALYSIS

It is well known that the stability limit $S_{\max}$ for solving Maxwell's equations can be given as [19]

$$S_{\max} = \frac{\lambda_T}{\lambda_S} \quad (15)$$

where λ_T is the temporal stability factor, and λ_S is the spatial stability factor.

The spatial stability factor can be written as

$$\lambda_S = \sqrt{Dim} \times W_s \quad (16)$$

where Dim is the dimension number. Considering that W_s with low-order differences are smaller than those with high-order differences, the second-order spatial difference can achieve maximum stability limit under the identical time strategy condition.

The temporal stability factor λ_T can be computed by solving the growth factor of the $\text{SFDTD}(p, q)$ schemes [13]. The λ_T of the symplectic integrators are also listed in Tables II and III.

For time-domain electromagnetic simulation, the required time step is directly proportional to $1/(\Delta_x S_{\max})$, every time step needs at least $m_{\min}$ iterations, and each iteration needs $O(1/\Delta_x^3)$ operations. Hence, total computational complexity is $O(1/(\Delta_x^4(S_{\max}/m_{\min})))$.

A novel averaged stability limit criterion can be defined as

$$\overline{S}_{\max} = \frac{S_{\max}}{m_{\min}} = \frac{\lambda_T/m_{\min}}{\lambda_S} = \frac{\overline{\lambda}_T}{\lambda_S} \qquad (17)$$

where $\overline{\lambda}_T$ is called the averaged temporal stability factor. Different from the stability limit $S_{\max}$ which focuses on "stable" algorithm, the averaged stability limit $\overline{S}_{\max}$ focuses on "efficient" algorithm. For the time-reversible symplectic integrators, c_1 can be combined with c_m, hence, $m_{\min} = m - 1$. Whereas, $m_{\min} = m$ for the half-unitary symplectic integrators.

The symplectic integrators with the same accuracy (especially for second-order accuracy) in time can be selected by the averaged temporal stability factor $\overline{\lambda}_T$. Tables II and III denote the chosen symplectic integrators with the asterisks. Moreover, as the order of the symplectic integrators increases, the averaged temporal stability factor decreases.

According to our survey, the maximum of $\overline{\lambda}_T$ is 2, which can be obtained by the m stage time-reversible symplectic integrators with $c_1 = c_m = 0.5/m_{\min}$, $c_l = 1/m_{\min}$, $l = 2, 3, \ldots m_{\min}$, $d_l = 1/m_{\min}$, $l = 1, 2, \ldots m_{\min}$, and $d_m = 0$. In particular, if we combine c_1 with c_m, all the symplectic integrators are equal. It can be verified that the time-reversible symplectic integrators only satisfy the first-order conditions and the second-order conditions. Hence, the leap-frog method can be implemented by the m stage time-reversible symplectic schemes with $\lambda_T = 2m_{\min}$ and $\overline{\lambda}_T = 2$. In [16], the authors drew a similar conclusion, but they did not seem to be aware that the symplectic schemes are equivalent to the second-order leap-frog time method.

In conclusion, the $\text{SFDTD}(2,2)$ scheme or the traditional $\text{FDTD}(2,2)$ method has the highest averaged stability limit $\overline{S}_{\max}$ in all the $\text{SFDTD}(p, q)$ schemes.

IV. COMPARISONS

A. Comparisons to Other High-Order Strategies

Using the fourth-order symplectic integrators denoted by the asterisk in Table II and the fourth-order centered spatial difference, the $\text{SFDTD}(4,4)$ scheme is compared with the original $\text{SFDTD}(4,4)$ scheme [13]. Using the same spatial difference and explicit fourth-order R-K approach [9], the R-K(4,4) approach is compared. In addition, the J-Fang(4,4) method [3] is also considered.

First, the stability limit $(S_{\max})$ of our scheme is 0.858 while 0.743 for the original scheme, 0.700 for the R-K(4,4) approach, and 0.577 for the J-Fang(4,4) method.

Second, the relative phase velocity error $(20 \log 10(Err))$ as a function of points per wavelength (PPW) for a plane wave traveling at $\theta = 60°$ and $\phi = 30°$ is shown in Fig. 1. Here, the CFL number is set to be 0.5.
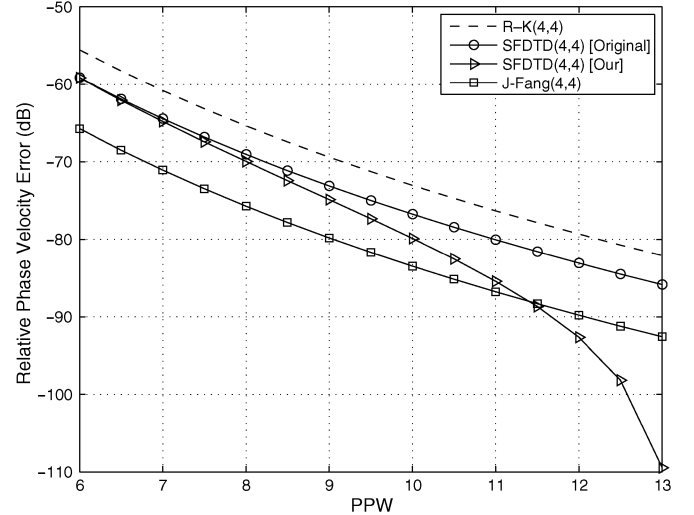
Fig. 1.   Dispersion curves for a plane wave traveling at $\theta = 60°$ and $\phi = 30°$ versus points per wavelength (PPW) discretization: $\text{CFL} = 0.5$.
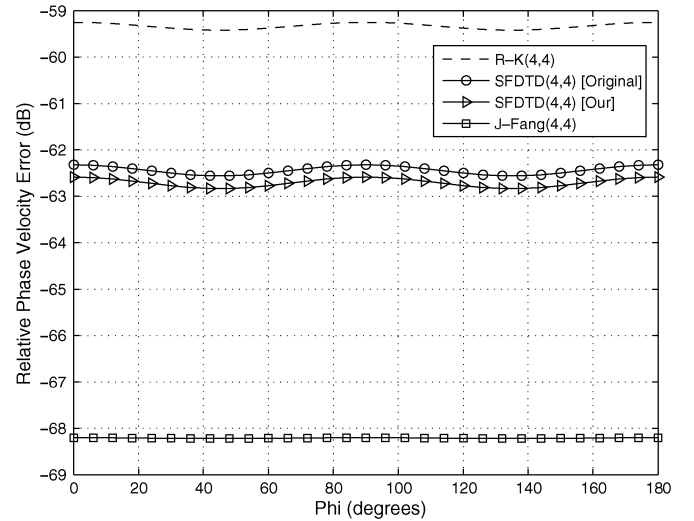
Fig. 2.   Dispersion curves for a plane wave traveling at $\theta = 30°$ versus the propagating angle ϕ: $\text{CFL} = 0.577$ and $\text{PPW} = 8$.

Third, the CFL number is reset to be 0.577, the spatial resolution is taken as 8 PPW, and the propagating angle $\theta = 30°$. We redraw the dispersion curves with respect to the propagating angle ϕ in Fig. 2.

From Figs. 1 and 2, one can notice that the J-Fang (4,4) method has the best numerical dispersion, and our scheme is superior to the original scheme and the R-K approach.

B. Low-Order Symplectic Integrators Versus High-Order Symplectic Integrators

Although the traditional $\text{FDTD}(2,2)$ method holds the highest averaged stability limit $\overline{S}_{\max}$, it is not the most efficient algorithm for optimum electromagnetic simulation, because of the unsatisfactory numerical dispersion. It has been verified that the staggered $\text{FDTD}(2,4)$ method demonstrates its advantages over the traditional $\text{FDTD}(2,2)$ method [4]. The advantages attribute to the utilization of high-order spatial difference.
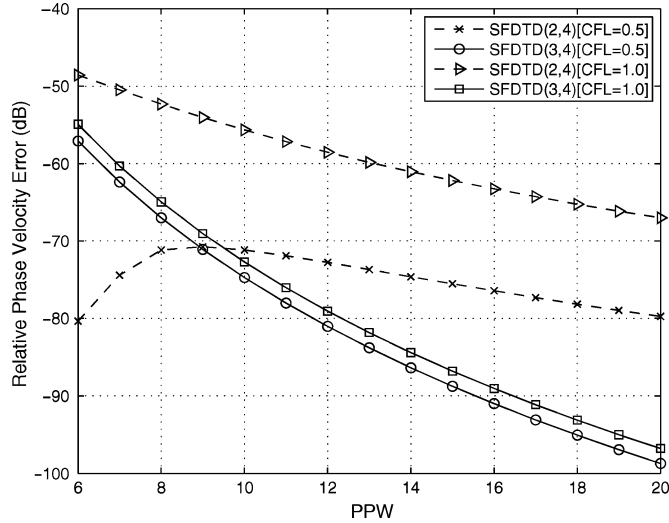
Fig. 3. Dispersion curves of the SFDTD(2,4) scheme and the SFDTD(3,4) scheme using different CFL number: $\theta = 45°$, $\phi = 0°$.

Fig. 4. Dispersion curves of the SFDTD(2,2) scheme and the SFDTD(3,2) scheme using different CFL number: $\theta = 45°$, $\phi = 0°$.

The problem of interest is whether the high-order time schemes have advantages over the low-order time schemes. The dispersion comparisons between the SFDTD scheme(2,4) and the SFDTD(3,4) scheme are given in Fig. 3. The SFDTD(2,4) scheme uses the time-reversible symplectic integrators constructed in Section III, and the SFDTD(3,4) scheme uses the half-unitary symplectic integrators denoted by the asterisk in Table III. In particular, the same iteration number $(m_{\min} = 3)$ and the same spatial differences are adopted. It can be clearly seen that the dispersion curves of the SFDTD(2,4) scheme go up drastically when the high CFL number is fixed. Contrarily, the dispersion curves of the SFDTD(3,4) scheme almost keep constant.

We change the fourth-order spatial difference to the second-order spatial difference, then redraw the dispersion curves of the SFDTD(2,2) scheme and the SFDTD(3,2) scheme in Fig. 4. Compared with the Fig. 3, the SFDTD(3,2) scheme dose not show any advantages over the SFDTD(2,2) scheme, no matter what CFL number we adopt.

Hence, high-order differences coupled to high-order symplectic integrators are effective for optimum electromagnetic simulation.

V. NUMERICAL RESULTS

A. One-Dimensional Propagation Problem

A Gaussian pulse can be defined by $\exp[-4\pi((t - t_0)/\tau)^2]$ with $t_0 = 10^{-8}$ s and $\tau = 1.33 \times 10^{-8}$ s. The space increment is set as $\Delta_z = 0.1$ m, and the CFL number is chosen to be 0.5. The time-domain waveforms are recorded in Fig. 5 after the pulse travels 10000 cells. Compared with the traditional FDTD(2,2) method and the staggered FDTD(2,4) method, the SFDTD(4,4) scheme agrees with the analytical solution very well.

B. Two-Dimensional Waveguide Problem

A two-dimensional waveguide resonator with size 2.286 cm × 1.016 cm is driven in TE_{21} mode. Calculated by the above mentioned SFDTD(4,4) scheme and the R-K (4,4) approach, the
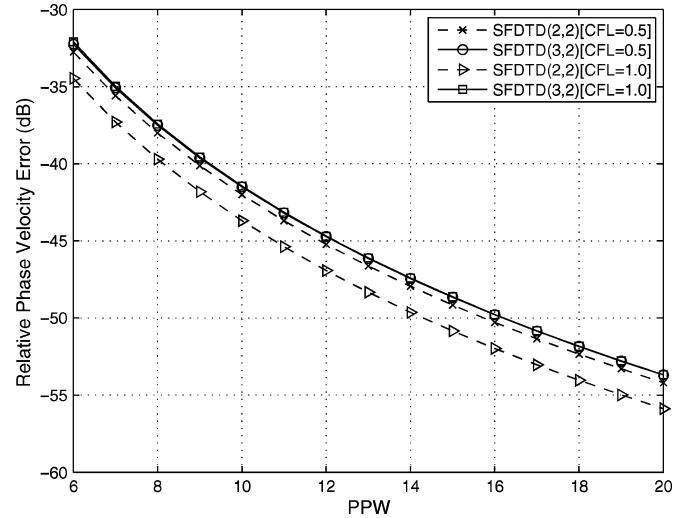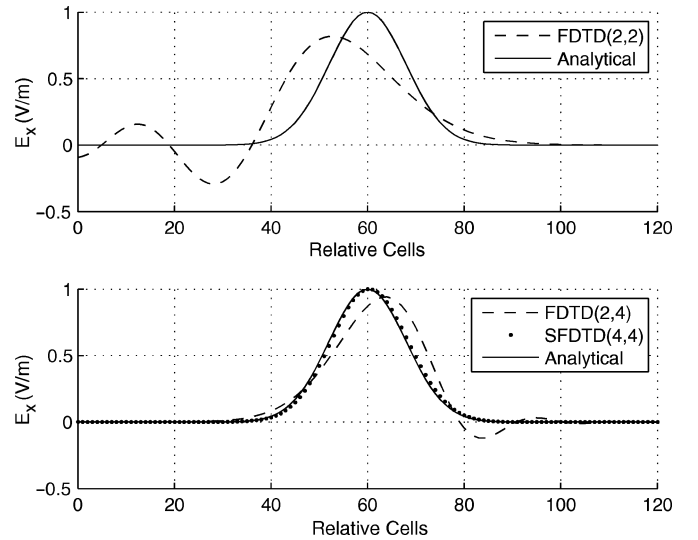
Fig. 5. Time-domain waveforms of the Gaussian pulse by the traditional FDTD(2,2) method, the staggered FDTD(2,4) method, and the SFDTD(4,4) scheme.

normalized averaged energy per three periods is drawn in Fig. 6. The uniform space increment $\Delta_\delta = 1.27$ mm, the CFL number is chosen to be 0.797, and the time step $n = 5100$. To obtain high-order accuracy, we use the analytical solution to treat the perfect electric conductor (PEC) boundary. Compared with the SFDTD(4,4) scheme, the R-K (4,4) approach has obvious amplitude error. Furthermore, within given numerical precision, the required memory of the R-K approach is four times more than that of the symplectic scheme.

C. Three-Dimensional Radiation Problem

The example on three-dimensional oscillating electric dipole is analyzed by kinds of symplectic schemes under the conditions of identical spatial differences and identical iteration number $(m_{\min} = 3)$. The computational domain occupies $67 \times 67 \times 67$ cells, the dipole is located at the source point k_s (33 1/2,33,33) near the center of the domain, and the recorded field point is
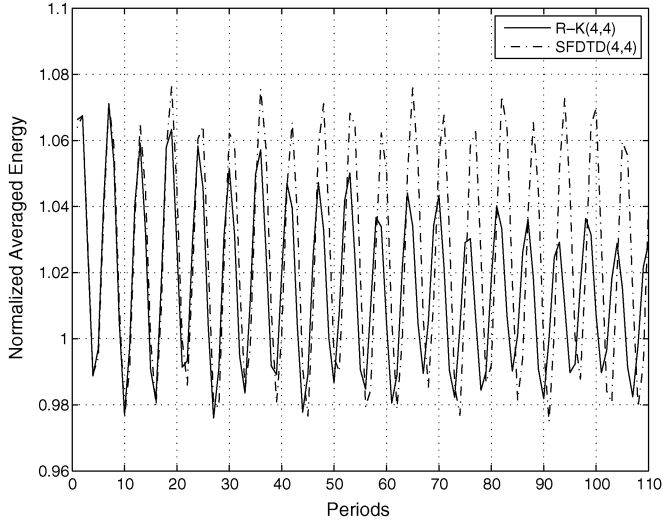
Fig. 6.   Normalized averaged energy of two-dimensional waveguide resonator calculated by the R-K(4,4) approach and the SFDTD(4,4) scheme.
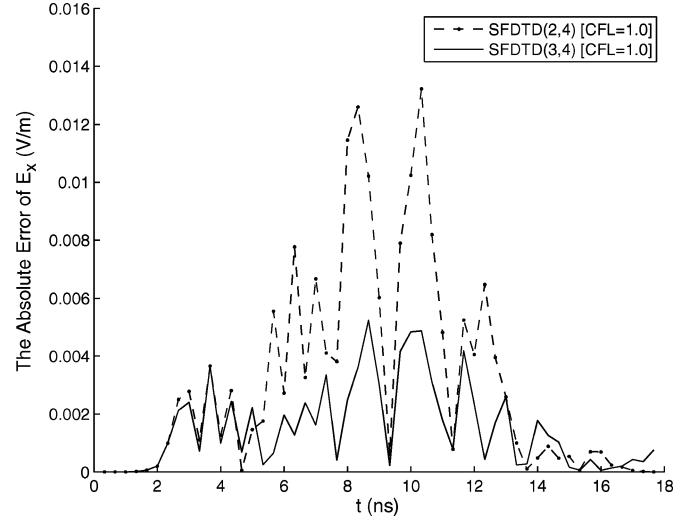
Fig. 8.   Absolute error of E_x field component computed by the SFDTD(2,4) scheme and the SFDTD(3,4) scheme: $\mathrm{CFL}_\delta = 1.0$.
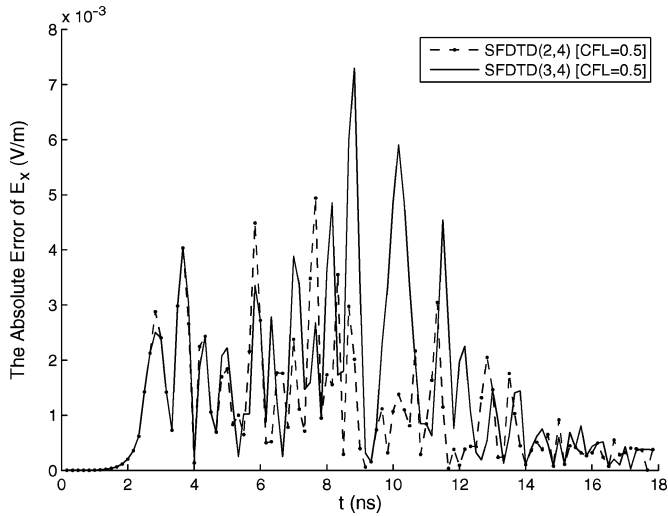
Fig. 7.   Absolute error of E_x field component computed by the SFDTD(2,4) scheme and the SFDTD(3,4) scheme: $\mathrm{CFL}_\delta = 0.5$.
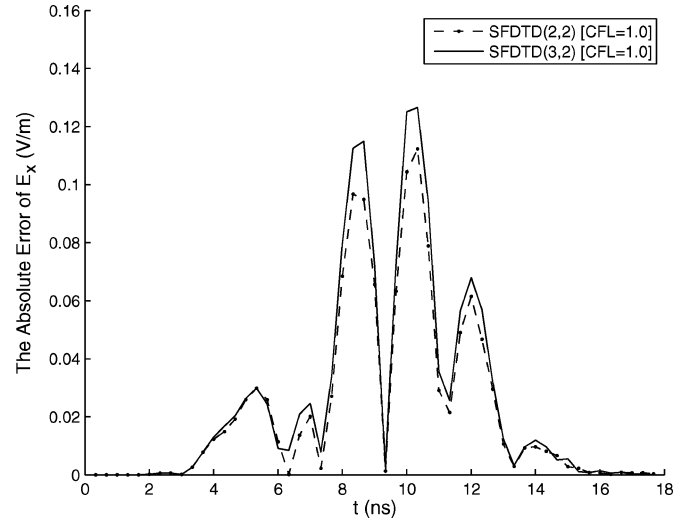
Fig. 9.   Absolute error of E_x field component computed by the SFDTD(2,2) scheme and the SFDTD(3,2) scheme: $\mathrm{CFL}_\delta = 1.0$.

located 10 cells from the source point. To absorb the outgoing wave, 10-layered perfectly matched layer (PML) is employed. Furthermore, the update equation for the electric dipole can be given by

$$E_x^{n+l/m}(k_s) = E_x^{n+l/m}(k_s) - 2 \times 10^{-10} d_l \times \mathrm{CFL}_\delta$$

$$\times \exp\left[-\left(\frac{(n+\tau_l)\Delta_t}{\tau_0} - 3 \right)^2 \right] \frac{[(n+\tau_l)\Delta_t - 3\tau_0]}{\tau_0^2 \Delta_\delta^2} \quad (18)$$

where $\tau_l = \sum_{r=1}^{l} c_r$, $\tau_0 = 2 \times 10^{-9}$ s, and $\Delta_\delta = 0.1$ m.

As shown in Fig. 7–9, the maximum absolute errors (L_1 errors) between the numerical results and the analytical solutions are provided for comparisons.

When the CFL number is taken as 0.5, the SFDTD(3,4) scheme does not show any advantages over the SFDTD(2,4) scheme. In Fig. 7, the L_1 errors for the SFDTD(3,4) scheme and the SFDTD(2,4) scheme are, respectively, 0.0073 and 0.0049.

However, when the CFL number is taken as 1.0, the SFDTD(3,4) scheme obtains more accurate result than the SFDTD(2,4) scheme. In Fig. 8, the L_1 errors for the SFDTD(3,4) scheme and the SFDTD(2,4) scheme are, respectively, 0.0052 and 0.0132. Obvious increase in L_1 error can be found by the SFDTD(2,4) scheme.

We change the fourth-order spatial difference to the second-order spatial difference, and the CFL number still is set to be 1.0. We can see that the SFDTD(3,2) scheme almost achieves the same numerical result as the SFDTD(2,2) scheme. In Fig. 9, the L_1 errors for the SFDTD(3,2) scheme and the SFDTD(2,2) scheme are, respectively, 0.127 and 0.112.

Therefore, matching the high-order symplectic integrators to high-order spatial differences is required for optimum electromagnetic simulation.
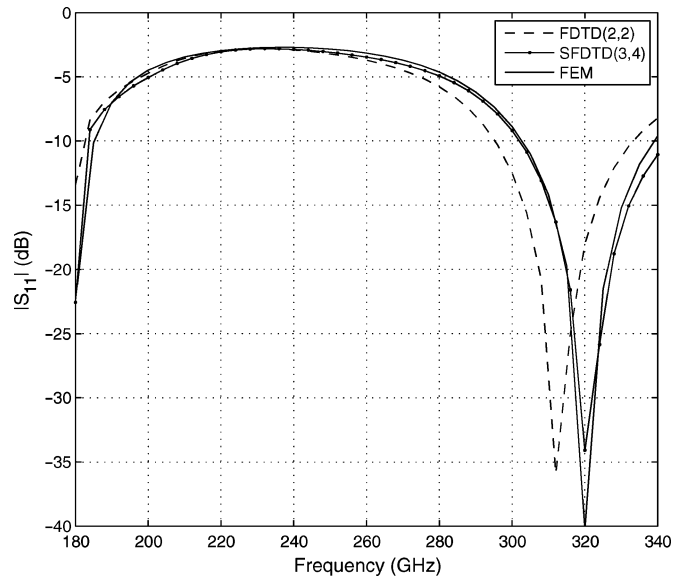
Fig. 10. S_{11} parameter of dielectric-filled waveguide calculated by the traditional FDTD(2,2) method and the SFDTD(3,4) scheme.

D. Three-Dimensional Wide-Band S-Parameter Extraction

Partially filled with dielectric of permittivity 3.7, the WR-3 optical waveguide is driven in the TE_{10} dominant-mode [20]. The size of the waveguide is 0.8636 mm × 0.4318 mm, and the length of the dielectric is 0.504 mm. The settings are taken as $\Delta_\delta = 0.072$ mm and $CFL_\delta = 0.5$. The ten layer PML is used to truncate the two waveguide ports, and sinusoidal-modulated Gaussian pulse is employed as excitation source. In particular, the PEC boundary is treated with the multiple image technique [21], and the air-dielectric interface is modeled by the scheme proposed in [22]. The wideband S-parameter is extracted after 5000 time steps. Compared with the traditional FDTD(2,2) method (see Fig. 10), the SFDTD(3,4) scheme can obtain satisfying numerical solution under coarse grid condition.

VI. CONCLUSION

The $\text{SFDTD}(p, q)$ schemes are the explicit and non-dissipative time-domain solvers for Maxwell's equations. First, the SFDTD schemes do not have amplitude error and save considerable memory compared with the R-K approaches. Second, it can achieve satisfying numerical stability and dispersion by selecting proper p and q. Third, to obtain accurate numerical results, the high p should be consistent with the high q. In addition, extremely high-order spatial differences are hard to treat inhomogeneous boundaries. Likewise, extremely high-order symplectic integrators cause low averaged stability limit or low computational complexity.

ACKNOWLEDGMENT

REFERENCES

[1] A. Taflove, *Computational Electrodynamics: The Finite-Difference Time-Domain Method*. Norwood, MA: Artech House, 1995.

[2] D. M. Sullivan, *Electromagnetic Simulation Using the FDTD Method*. New York: IEEE Press, 2000.

[3] J. Fang, "Time domain finite difference computation for Maxwell's equations," Ph.D. dissertation, Univ. California, Berkeley, CA, 1989.

[4] A. Yefet and P. G. Petropoulos, "A staggered fourth-order accurate explicit finite difference scheme for the time-domain Maxwell's equations," *J. Comput. Phys.*, vol. 168, pp. 286–315, Apr. 2001.

[5] S. V. Georgakopoulos, C. R. Birtcher, C. A. Balanis, and R. A. Renaut, "Higher-order finite-difference schemes for electromagnetic radiation, scattering, and penetration, Part I: Theory," *IEEE Antennas Propag. Mag.*, vol. 44, pp. 134–142, Feb. 2002.

[6] S. V. Georgakopoulos, C. R. Birtcher, C. A. Balanis, and R. A. Renaut, "Higher-order finite-difference schemes for electromagnetic radiation, scattering, and penetration, Part 2: Applications," *IEEE Antennas Propag. Mag.*, vol. 44, pp. 92–101, Apr. 2002.

[7] A. Taflove, *Advances in Computational Electrodynamics: The Finite-Difference Time-Domain Method*. Norwood, MA: Artech House, 1998.

[8] J. L. Young, D. Gaitonde, and J. S. Shang, "Toward the construction of a fourth-order difference scheme for transient EM wave simulation: Staggered grid approach," *IEEE Trans. Antennas Propag.*, vol. 45, pp. 1573–1580, Nov. 1997.

[9] J. S. Shang, "High-order compact-difference schemes for time-dependent Maxwell equations," *J. Comput. Phys.*, vol. 153, pp. 312–333, Aug. 1999.

[10] T. Namiki, "A new FDTD algorithm based on alternating-direction implicit method," *IEEE Trans. Microw. Theory Tech.*, vol. 47, pp. 2003–2007, 1999.

[11] Z. Fenghua, C. Zhizhang, and Z. Jiazong, "Toward the development of a three-dimensional unconditionally stable finite-difference time-domain method," *IEEE Trans. Microw. Theory Tech.*, vol. 48, pp. 1550–1558, 2000.

[12] J. M. Sanz-Serna and M. P. Calvo, *Numerical Hamiltonian Problems*. London, U.K.: Chapman and Hall, 1994.

[13] T. Hirono, W. Lui, S. Seki, and Y. Yoshikuni, "A three-dimensional fourth-order finite-difference time-domain scheme using a symplectic integrator propagator," *IEEE Trans. Microw. Theory Tech.*, vol. 49, pp. 1640–1648, Sep. 2001.

[14] R. Rieben, D. White, and G. Rodrigue, "High-order symplectic integration methods for finite element solutions to time dependent Maxwell equations," *IEEE Trans. Antennas Propag.*, vol. 52, pp. 2190–2195, 2004.

[15] M. Kusaf, A. Y. Oztoprak, and D. S. Daoud, "Optimized exponential operator coefficients for symplectic FDTD method," *IEEE Microw. Wireless Compon. Lett.*, vol. 15, pp. 86–88, Feb. 2005.

[16] M. Kusaf and A. Y. Oztoprak, "Higher stability limits for the symplectic FDTD method by making use of Chebyshev polynomials," *IEEE Microw. Wireless Compon. Lett.*, vol. 16, pp. 579–581, Nov. 2006.

[17] H. Yoshida, "Construction of higher order symplectic integrators," *Physica D: Nonlinear Phenomena*, vol. 46, pp. 262–268, Nov. 1990.

[18] S. K. Gray and D. E. Manolopoulos, "Symplectic integrators tailored to the time-dependent Schrödinger equation," *J. Chem. Phys.*, vol. 104, pp. 7099–7112, May 1996.

[19] S. Zhao and G. W. Wei, "High-order FDTD methods via derivative matching for Maxwell's equations with material interfaces," *J. Comput. Phys.*, vol. 200, pp. 60–103, Oct. 2004.

[20] D. V. Krupezevic, V. J. Brankovic, and F. Arndt, "Wave-equation FD-TD method for the efficient eigenvalue analysis and S-matrix computation of waveguide structures," *IEEE Trans. Microw. Theory Tech.*, vol. 41, pp. 2109–2115, 1993.

[21] Q. S. Cao, Y. C. Chen, and R. Mittra, "Multiple image technique (MIT) and anistropic perfectly matched layer (APML) in implementation of MRTD scheme for boundary truncations of microwave structures," *IEEE Trans. Microw. Theory Tech.*, vol. 50, pp. 1578–1589, Jun. 2002.

[22] W. Sha, Z. X. Huang, X. L. Wu, and M. S. Chen, "Application of the symplectic finite-difference time-domain scheme to electromagnetic simulation," *J. Comput. Phys.*, vol. 225, pp. 33–50, Jul. 2007.
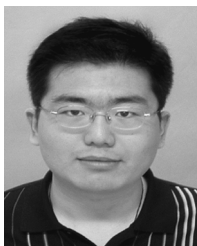
Wei Sha was born in Suzhou, Anhui Province, China, in 1982. He received the B.S. degree in electronic engineering from Anhui University, Hefei, China, in 2003, where he is currently working toward the Ph.D. degree.

His current research interests include time-domain numerical methods and signal processing.

Mingsheng Chen was born in Nanling, Anhui Province, China, in 1981. He received the B.S. degree in applied mathematics from Anhui University, Hefei, China, in 2003, where he is currently working toward the Ph.D. degree.

His current research interests include frequency-domain numerical methods and wavelet theory.

Zhixiang Huang was born in Guangde, Anhui Province, China, in 1979. He received the B.S. degree in mathematical statistics and the Ph.D. degree in electromagnetic scattering, inverse scattering, and target identification from Anhui University, Hefei, China, in 2002 and 2007, respectively.

His current research interests include time-domain numerical methods and parabolic equation method.

Xianliang Wu was born in Bozhou, Anhui Province, China, in 1955. He received the B.S. degree in electronic engineering from Anhui University, Hefei, China, in 1982.

He is a Full Professor in the Department of Electronic Engineering and is the Director of the Laboratory of Electromagnetic Field and Microwave Technology at Anhui University and is also the Principal of Hefei Teachers College. He has authored or coauthored more than 70 papers and two books. His current research interests include electromagnetic field theory, electromagnetic scattering and inverse scattering, wireless communication, etc.

Prof. Wu is a senior member of the Chinese Institute of Electronics, and an Associate Director of the Chinese Institute of Microwave Measurement. He received the Ministry of Education Award for Science and Technology Progress and the Science and Technology Award of Anhui Province.